

The scattering from generalized Cantor fractals

A. Yu. Cherny,¹ E. M. Anitas,^{1,2} A. I. Kuklin,¹ M. Balasoiu,^{1,3} and V. A. Osipov¹

¹*Joint Institute for Nuclear Research, Dubna 141980, Russia*

²*Physics Department, The West University of Timisoara, Blvd. V. Parvan 4, Timisoara 300223, Romania*

³*Horia Hulubei National Institute of Physics and Nuclear Engineering, RO-077125 Bucharest-Magurele, Romania*

(Dated: February 7, 2020)

We suggest a three dimensional generalization of well-known triadic Cantor fractal in one dimension. Its fractal dimension is controlled with a cut-off parameter and can vary from 0 to 3. The intensity profile of a small-angle scattering from the generalized Cantor fractals is calculated. The considered system is generated by a set of iterative rules, each iteration corresponds to a certain fractal generation. A small-angle scattering is considered from the monodisperse sets being randomly oriented and placed. The scattering intensities represent minima and maxima superimposed on a power law decay with the exponent being equal to the fractal dimension of the scatterer, but the minima and maxima are damped with increasing polydispersity of the fractal sets. It is shown that for a finite generation of the fractals, the exponent value changes at sufficiently large wave vectors from the fraction dimension to 4, the value given by the usual Porod law. It is shown that the number of particles, from which the fractal is composed, can be estimated from the value of the boundary between the fractal and Porod region. The radius of gyration of the fractal is calculated analytically.

PACS numbers: 61.43.Hv, 61.05.fg, 61.05.cf

Keywords: nonrandom fractals, Cantor set, SANS, SAXS

I. INTRODUCTION

Small-angle scattering (X-rays, light, neutrons) [1, 2, 3] is one of the most important investigation technique for structural properties of fractal systems [4, 5, 6, 7] at nanometer scale. This technique yields the Fourier transform of the spatial density distribution of a studied system within the wave vector magnitude from 10^{-4} to 10^{-1}\AA^{-1} and thus is very effective for the object size from 10 to 10^4\AA [8]. Since only a finite range in the wave vector space is available experimentally, the interpretation of results requires theoretical models.

While in the case of non-deterministic (random) fractals, different models for mass and surface fractals [9, 10, 11, 12, 13, 14] have been successfully developed and applied to a variety of materials [15], for deterministic fractals, rather few attempts were made [16, 17, 18]. This is probably due to technological limitations encountered until several years ago in preparation of the fractal-like structures. Now modern experimental techniques for obtaining deterministic fractal systems were developed [19, 20, 21]. The small-angle neutron scattering (SANS) from self-assembled porous silica materials [19] was carried out in Ref. [22]. A molecular Sierpinski hexagonal gasket, the deterministic fractal polymer, was also obtained by chemical methods [23].

A main indicator of the fractal structure is the power law behaviour of the scattering curve

$$I(q) \sim q^{-\alpha} \quad (1)$$

where α is the power law scattering exponent. It carries information regarding the fractal dimension of the scatterer [9, 10, 11, 12, 13, 14, 24]: $\alpha = D$ for mass fractals and $\alpha = 6 - D$ for surface fractals. One can write down even a more general expression [25] for the exponent in a two phase geometrical configuration, where one phase is a mass fractal of fractal dimension D_m with pores inside of fractal dimension D_p ; besides, the boundary surface between the phases

also forms a fractal of dimension D_s . Then the exponent reads $\alpha = 2(D_m + D_p) - D_s - 6$. In a particular case of a mass fractal we have $D_s = D_m < 3$ and $D_p = 3$, while for a surface fractal $D_m = D_p = 3$ and $2 < D_s < 3$.

Construction of nonrandom fractal models usually assumes the presence of a generator divided in subparts. Then some of them are removed according to an iterative rule and the process is repeated for each remaining part, whose form factor is computed for each iteration.

By contrast to the simple power law behaviour (1), scattering from nonrandom fractals, like Menger sponge, fractal jack [16] or from other surface like type [18], show a successive superposition of maxima and minima decaying as a power law, which can be called generalized power law. This is due to a spatial order in nonrandom fractals: the scattering curve $I(q)$, being the Fourier transform of the pair distribution function, oscillates by reason of singularities in this function or its derivatives. If there is a disorder in the system then the singularities are smeared out as in the case of random fractals, whose behaviour follows the power law (1). On the other hand, real physical systems always exhibit a specific kind of disorder, polydispersity. Below we show that when a polydispersity of nonrandom fractals is taken into account, these local oscillations cancel out with increasing the width of the distribution function. This is consistent with the results obtained for a similar fractal, Menger sponge, by averaging over a Schulz distribution function [26].

The existing models [16, 18] assume the given fractal dimensions that imposes some restrictions on applying the models to real systems. In this paper, a generalization of Cantor sets are proposed that allows us to control the fractal dimension with a cut-off parameter. The scattering intensity of randomly oriented generalized Cantor sets are obtained analytically for monodisperse and polydisperse systems. Our method is based on the approach that was successfully employed in some aspects for other similar systems of non-random fractals

like Menger sponge [16].

Numerous examples of the fractal-like behaviour were obtained experimentally in collaboration with one of the authors of this paper (A.I.K.) for different kind of objects: soils [27, 28, 29], biology objects [30], and nanocomposites [31]. Only three parameters are extracted from the fractal scattering intensity: its exponent α [see Eq. (1)] and the edges of the fractal region in q -space, which appear as "knees" in the scattering line in the logarithmic scale; other parameters are not usually obtained from the SANS curves.

If some features of the fractal structure are available from other considerations, one can construct a model and get an additional information about the fractal parameters. Note that a real physical system does not possess an infinite scaling effect and the number of iterations is always finite. In this paper we calculate the scattering from the generalized Cantor sets for a finite number of iterations. As discussed below, many features of the scattering are quite general; in particular, one can estimate the number of particles, from which the fractal is formed.

II. CONSTRUCTION OF THE GENERALIZED CANTOR SET

The generalized Cantor set can be constructed from the homogeneous cube by iterations, which we will call approximants. The zero order iteration (generator) is the cube itself with the side length l_0 , which can be specified in the Cartesian coordinate as a set of points obeying the conditions $-l_0/2 \leq x \leq l_0/2$, $-l_0/2 \leq y \leq l_0/2$, $-l_0/2 \leq z \leq l_0/2$. The first iteration removes all the points from the cube with coordinates $-\gamma l_0/2 < x < \gamma l_0/2$ or $-\gamma l_0/2 < y < \gamma l_0/2$ or $-\gamma l_0/2 < z < \gamma l_0/2$. The dimensionless cut-off parameter γ can take any value between 0 and 1. Thus, the initial cube is divided into twenty seven parts, the eight cubes left in the corners, with the length of the edge $(1 - \gamma)l_0/2$, and the nineteen parallelepipeds removed, see Fig. 1 (upper panel). In order to obtain the second approximant, one should do the same with each of the eight cubes, thus leaving the sixty eight cubes of the side length $(1 - \gamma)^2 l_0/4$. It is not difficult to see that the m th approximant to the three-dimensional Cantor set is composed of the $N_m = 8^m$ cubes of the side length

$$l_m = (1 - \gamma)^m l_0 / 2^m. \quad (2)$$

The generalized Cantor set is obtained in the limit $m \rightarrow \infty$.

The Hausdorff dimension [5] of the set can be determined from the intuitively apparent relation $N_m \sim (l_0/l_m)^D$ at large number of iterations, which yields

$$D = \lim_{m \rightarrow \infty} \frac{\ln N_m}{\ln(l_0/l_m)} = -\frac{3 \ln 2}{\ln \beta_s}, \quad (3)$$

where the scaling factor $0 < \beta_s < 1$ for each iteration is defined as

$$\beta_s \equiv (1 - \gamma)/2. \quad (4)$$

In the same manner, we obtain that the fractal dimension of the surface coincides with that of the bulk structure. Then, we

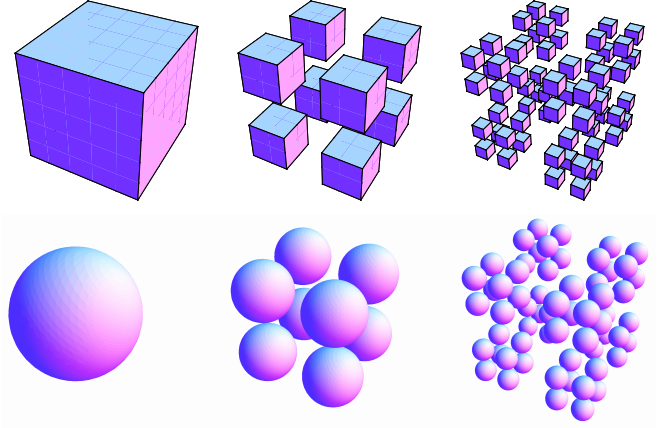


FIG. 1: Zero, first, and second iterations (approximants) for the generalized Cantor set, composed of cubes (upper panel) and balls (lower panel).

have a mass fractal whose dimension can be varied between the values of zero and three by changing the parameter γ .

One can generalize the fractal construction replacing the cubes by any solid three-dimensional shapes and using the same scaling (4) for each iteration. For example, a ball of arbitrary radius $R \leq l_0/2$ in the center of the cell can be used as a generator instead of the initial cube, see Fig. 1 (lower panel). One can see that the fractal dimension is still given by Eq. (3).

III. FORMFACTOR OF THE MONODISPERSE SET

A. General remarks

We consider a two phase system of particles, consisting of small pieces of "mass". The "masses" are embedded into a solid matrix, which can be associated with the "pores" discussed in Sec. I. The particles are also immersed into the solid matrix or dissolved in a solution of the same density of scattering length. The scattering length densities are ρ_m for the "mass" and ρ_p for the "pores". They are determined by the relation $\rho \equiv \sum_i b_i / \Delta V$, where summation is over the scattering centers located in the volume ΔV . The difference $\rho_m - \rho_p$ is called scattering contrast. In what follows, we mean by particle the m th approximant to the generalized Cantor set.

The neutron scattering cross section per unit volume of the sample is given by [1]

$$\frac{1}{V'} \frac{d\sigma}{d\Omega} = n(\rho_m - \rho_p)^2 V^2 \langle |F(\mathbf{q})|^2 \rangle, \quad (5)$$

where \mathbf{q} is momentum transfer, n is number of particles per unit volume and V is the total volume of the "mass" in the particle. The normalized scattering formfactor is defined as [32]

$$F(\mathbf{q}) \equiv \frac{1}{V} \int_V e^{-i\mathbf{q} \cdot \mathbf{r}} d\mathbf{r}, \quad (6)$$

and the symbol $\langle \dots \rangle$ denotes the mean value over all the orientations of the particle. Here we assume that the particles are randomly oriented in space and their positions are not correlated. The latter means that we neglect the particle interactions and put the interparticle structure factor equal one, which is quite reasonable if the average distance between the particles is sufficiently large.

If the probability of any orientation is the same then the mean value can be calculated by averaging over all the directions \mathbf{n} of momentum transfer $\mathbf{q} = q\mathbf{n}$, that is, integrate over the solid angle in the spherical coordinates $q_x = q \cos \varphi \sin \vartheta$, $q_y = q \sin \varphi \sin \vartheta$, and $q_z = q \cos \vartheta$

$$\langle f(q_x, q_y, q_z) \rangle \equiv \frac{1}{4\pi} \int_0^\pi d\vartheta \sin \vartheta \int_0^{2\pi} d\varphi f(q, \vartheta, \varphi). \quad (7)$$

Once we know the absolute values of the intensity (5), the concentration of the fractals and the contrast, we can obtain the fractal volume from the scattering at zero momentum.

B. The fractal formfactor

One can easily obtain an explicit analytical formula for formfactor (6) of the m th approximant. Similar method for obtaining the formfactor of nonrandom fractals was used in Ref. [16] (see also a generalization in Ref. [33]). In zero order, the particle is a generator with formfactor $F_0(\mathbf{q})$. If the generator is a cube of the edge l_0 we have $F_0 = F_c$, where

$$F_c(\mathbf{q}) = \frac{\sin(q_x l_0/2)}{q_x l_0/2} \frac{\sin(q_y l_0/2)}{q_y l_0/2} \frac{\sin(q_z l_0/2)}{q_z l_0/2}. \quad (8)$$

In the case of the ball of radius R , we have $F_0 = F_b$ with

$$F_b(\mathbf{q}) = 3 \frac{\sin(qR) - qR \cos(qR)}{(qR)^3}, \quad q = |\mathbf{q}|. \quad (9)$$

For obtaining the first order formula, one can use two simple properties of the the scattering formfactor (6) for a particle of arbitrary shape:

- i) If we scale all the length of a particle as $l \rightarrow \beta l$ then $F(\mathbf{q}) \rightarrow F(\beta \mathbf{q})$.
- ii) If a particle is translated $\mathbf{r} \rightarrow \mathbf{r} + \mathbf{a}$ then $F(\mathbf{q}) \rightarrow F(\mathbf{q}) \exp(-i\mathbf{q} \cdot \mathbf{a})$.
- iii) If a particle consists of two not overlapping subsets I and II, then $F(\mathbf{q}) = (V_I F_I(\mathbf{q}) + V_{II} F_{II}(\mathbf{q})) / (V_I + V_{II})$.

The first approximant consists of the eight cubes (balls), which differ from the initial cube by the scaling factor (4) and whose center positions are shifted from the center of the initial cube by the vectors $\mathbf{a}_j = \{\pm \beta_t l_0, \pm \beta_t l_0, \pm \beta_t l_0\}$ with various combinations of the signs. Here we put by definition

$$\beta_t \equiv (1 + \gamma)/4. \quad (10)$$

Using the definition (6) and the properties i), ii), and iii), we obtain

$$V_1 F_1(\mathbf{q}) = \sum_{j=1}^8 \beta_s^3 V_0 F_0(\beta_s \mathbf{q}) \exp(-i\mathbf{q} \cdot \mathbf{a}_j). \quad (11)$$

Here total volume of the first approximant is given by $V_1 = 8V_0\beta_s^3$, and V_0 is the volume of the initial cube (ball). Writing down the sum explicitly yields

$$F_1(\mathbf{q}) = G_1(\mathbf{q}) F_0(\beta_s \mathbf{q}), \quad (12)$$

where we introduce the function by definition

$$G_1(\mathbf{q}) \equiv \cos(q_x l_0 \beta_t) \cos(q_y l_0 \beta_t) \cos(q_z l_0 \beta_t). \quad (13)$$

For the second approximant we repeat the same operation on $F_1(\mathbf{q})$ and obtain

$$F_2(\mathbf{q}) = G_1(\mathbf{q}) F_1(\beta_s \mathbf{q}) = G_1(\mathbf{q}) G_1(\beta_s \mathbf{q}) F_0(\beta_s^2 \mathbf{q}). \quad (14)$$

In the same manner, we infer the general relation

$$F_m(\mathbf{q}) = P_m(\mathbf{q}) F_0(\beta_s^m \mathbf{q}), \quad (15)$$

where

$$P_m(\mathbf{q}) \equiv G_1(\mathbf{q}) G_2(\mathbf{q}) \dots G_m(\mathbf{q}), \quad (16)$$

$$G_m(\mathbf{q}) \equiv \cos(q_x l_0 \beta_t \beta_s^{m-1}) \cos(q_y l_0 \beta_t \beta_s^{m-1}) \times \cos(q_z l_0 \beta_t \beta_s^{m-1}) \quad (17)$$

for $m = 1, 2, \dots$. We can also put by definition $G_0(\mathbf{q}) = 1$ and $P_0(\mathbf{q}) = 1$ in order to describe the generator.

To obtain the cross section given by Eq. (5), we should calculate the mean value of $|F_m(\mathbf{q})|^2$ over all the directions \mathbf{n} of momentum transfer with formula (7)

$$I_m(q l_0) \equiv \langle |F_m(\mathbf{q})|^2 \rangle, \quad (18)$$

where $m = 0, 1, \dots$. Here the formfactor $F_m(\mathbf{q})$ is given by Eqs. (15)-(17) in conjunction with Eqs. (4) and (10); the initial formfactor F_0 is represented by Eq. (8) or (9). Note that the intensity (18) of the m th monodisperse approximant depends on the wavevector and the initial length through the product $q l_0$ only. The results for first three iterations are shown in Fig. 2.

C. Discussion of the results

These results are in accordance with scattering from similar systems like Menger sponge, displaying the same behaviour of the scattering curve [16]. The authors of Ref. [16], first, omitted the last multiplier in Eq. (15), assuming that $q l_0 \beta_s^m \ll 1$, and, second, used the expansion of cosines that allows for reducing the intensity formula to a sum of quite simple terms. However, the number of the terms grows exponentially with increasing the number of iterations, and the method becomes very time-consuming even for $m > 4$. By contrast, using the straightforward integration in Eq. (18), we can employ the exact relation (15) for arbitrary m , which can yield a substantial improving of the accuracy. At sufficiently large $q l_0$, the main contribution to the integral comes from a few number of narrow and high spikes, which is typical for an interference pattern. Nevertheless, the integral can be evaluated even at sufficiently large values of $q l_0$, up to 10^4 .

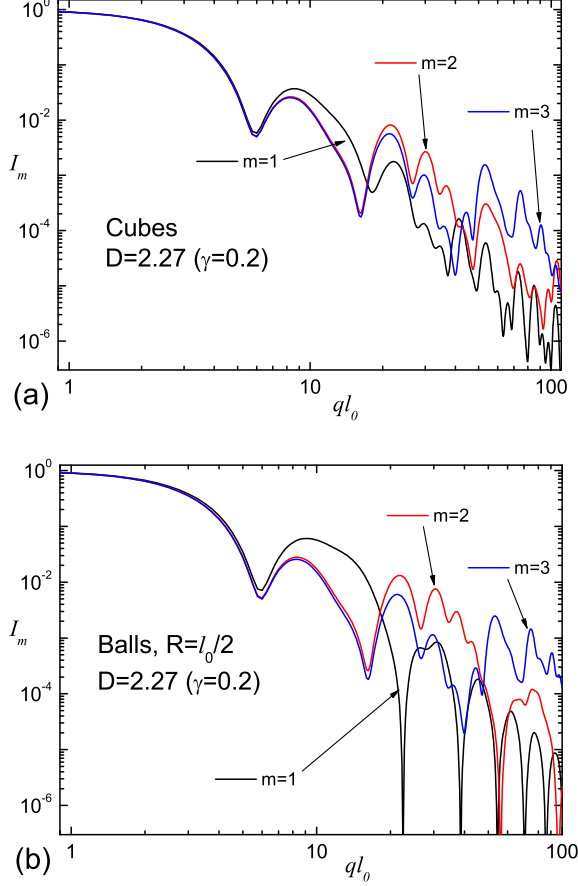


FIG. 2: Scattering intensities (18) for first three iterations of the generalized Cantor set composed from cubes (a) and balls (b). Radius of the initial ball (generator) is $R = l_0/2$. The intensities can be estimated as a product of the fractal structure factor (20) and scaled zero iteration, shown in Fig. 3.

1. The fractal structure factor

The scattering intensity can be approximately represented as

$$I_m(ql_0) \simeq S_m(q) \langle |F_0(\beta_s^m \mathbf{q})|^2 \rangle, \quad (19)$$

$$S_m(q) \equiv \langle |P_m(\mathbf{q})|^2 \rangle. \quad (20)$$

We will call this quantity formfactor of the fractal [34]. It is nothing but the intensity (18) with $F_0 = 1$; for instance, it happens when the radius of the ball tends to zero. The formfactor of ball (9) is isotropic; hence, relation (19) is satisfied exactly. The structure factor carries information about the relative positions of the cubes (balls) in the fractal. Indeed, using the definition (6) and the analytical formula for the formfactor (15), one can obtain

$$P_m(\mathbf{q}) = \frac{1}{N_m} \sum_{1 \leq j \leq N_m} \exp[-i\mathbf{r}_j^{(m)} \cdot \mathbf{q}]. \quad (21)$$

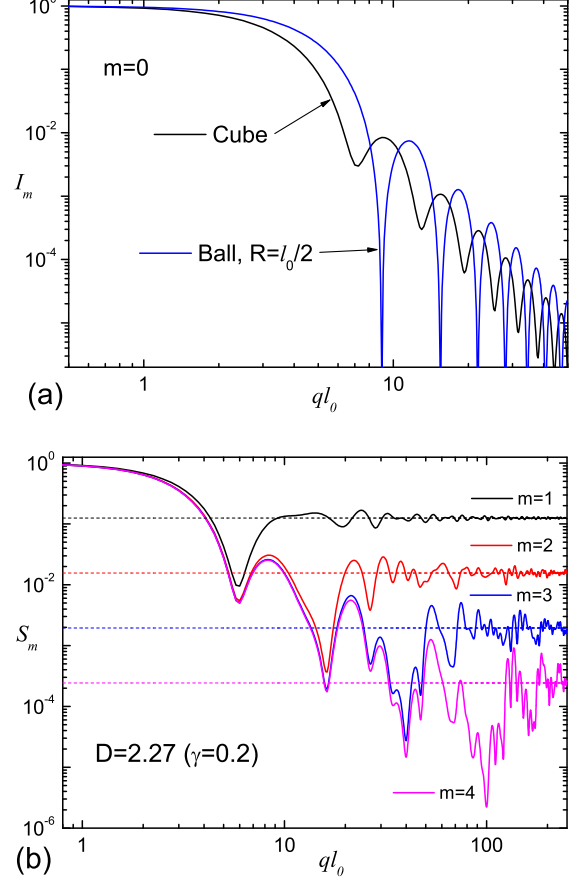


FIG. 3: Scattering intensities (18) for various system geometries. (a) Zero iteration: the intensities for the cube with edge l_0 and the ball of radius $R = l_0/2$. (b) The structure factor of the generalized Cantor fractal given by Eq. (20) [or by Eq. (18) with $F_0(\mathbf{q}) = 1$]. The diagram represents first four iterations at $\gamma = 0.2$, which corresponds to the fractal dimension $D \simeq 2.27$. The asymptotics for the structure factor of the m th iteration is given by the inverse total number of cubes(balls) $1/8^m$, when $ql_0 \gtrsim 1/\beta_s^m$, see discussion in the text.

Here $N_m = 8^m$ is the total number of cubes (balls) in the m th iteration, and $\mathbf{x}_j^{(m)}$ are their center-of-mass coordinates. Then the fractal structure factor (20) reads

$$S_m(q) = \frac{1}{N_m} + \frac{1}{N_m^2} \sum_{1 \leq k < j \leq N_m} \frac{\sin q r_{jk}^{(m)}}{q r_{jk}^{(m)}}, \quad (22)$$

$$r_{ik}^{(m)} \equiv |\mathbf{r}_j^{(m)} - \mathbf{r}_k^{(m)}|. \quad (23)$$

Deriving the last relation, we use formula $\langle \exp(i\mathbf{a} \cdot \mathbf{q}) \rangle = \sin(aq)/(aq)$, which follows from Eq. (7). Let us analyze the obtained formulas. At sufficiently large momentum, Eq. (22) yields the asymptotics

$$S_m(q) \simeq 1/8^m, \quad (24)$$

see Fig. 3. The underlying physics is quite clear: when the reciprocal wavevector is smaller than the characteristic variance

of the distance between the points then the scattering pattern does not “feel” their spatial correlations. The characteristic valiance is of order $ql_0\beta_t\beta_s^m \sim ql_0\beta_s^m$, and the asymptotics is attained when

$$ql_0 \gg 1/\beta_s^m. \quad (25)$$

2. Generalized power law

As was noted in Sec. I, rigid spatial correlations between the points in the nonrandom fractal yield singularities in the form of δ -functions, which leads to oscillations in the structure factor, see Fig. 3b. The weight of each δ -functions follows the power law with respect to the distance between points $r_{ik}^{(m)}$, as determined by the fractal dimension. As a consequence, the scattering curve shows groups of maxima and minima which are superimposed on a monotonically decreasing curve proportional to a power of the absolute value of scattering vector (generalized power law). Short-distance correlations govern the long-range wave vector oscillations, and vice versa. It is essential that the oscillations are not damped with increasing the number of iterations, because it influences only on the short-range correlations and, hence, the scattering behaviour at large momentum.

An advantage of the considered model is explicit analytical expressions (15)-(17), which allow us to estimate easily the fractal region where the generalized power law takes place. If the cosine argument in G_{m+1} is much smaller than one, then further increasing of m does not lead to an essential correction and the m th iteration reproduces the intensity that the ideal Cantor fractal would give at this argument. Thus, the m th iteration works well within the region $ql_0\beta_s^m \ll 1$, where we use the estimation $\beta_t \sim 1$. Such a behaviour can be seen in Fig. 2.

On the other hand, within the Guinier region $ql_0 \lesssim 1$ the intensity is very close to one and we have a plateau in the logarithmic scale. Then the generalized power-law behaviour is observed in the region

$$1 \ll ql_0 \ll 1/\beta_s^m. \quad (26)$$

This estimation indicates two typical length scales, important for fractal, its size l_0 and the characteristic distance inside the m th iteration $l_0\beta_s^m$ [18]. In the fractal region $F_0(\mathbf{q}) \simeq 1$, and we obtain from Eq. (19)

$$I_m(ql_0) \simeq S_m(q). \quad (27)$$

Beyond the fractal region, when inequality (25) is satisfied, we derive from Eq. (24)

$$I_m(ql_0) \simeq \langle |F_0(\beta_s^m \mathbf{q})|^2 \rangle / 8^m. \quad (28)$$

It follows that beyond the fractal region, the scattering intensity resembles the intensity of the generator (that is, cube or ball in our case), see Fig. 4. In particular, the maximums of the curve obey the Porod law [3].

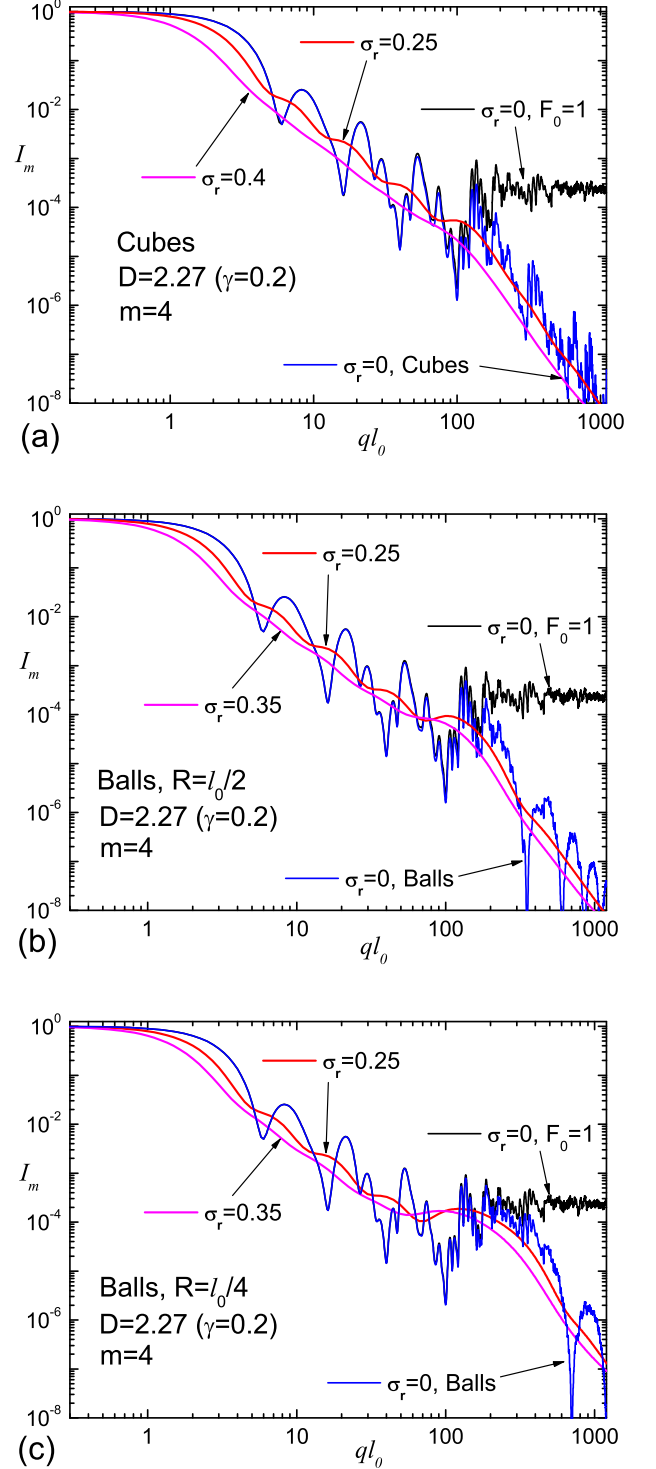


FIG. 4: Influence of polydispersity on the scattering from the Cantor fractals of cubes (a) and balls (b,c). Radius of the initial ball (generator) is $R = l_0/2$ (b) and $R = l_0/4$ (c). The upper monodisperse curve is the structure factor (20) that in the fractal region $1 \lesssim ql_0 \lesssim 1/\beta_s^m$ coincides with the exact intensity (18). In the fractal region, the exponent of the polydisperse curve equals the fractal dimension. While at large momentum $ql_0 \gtrsim 1/\beta_s^m$ the power law exponent changes from the fractal exponent to 4, given by the usual Porod law.

3. The radius of gyration

One can calculate the radius of gyration R_g of the fractal. By definition [1], in the Guinier region $I(q) = I(0)(1 - q^2 R_g^2/3 + \dots)$. Expanding Eq. (15) as a power series in q and substituting the result into Eq. (18) yields

$$R_g = \sqrt{\beta_s^{2m} R_{g0}^2 + 3\beta_t^2 \frac{1 - \beta_s^{2m}}{1 - \beta_s^2} l_0^2}, \quad (29)$$

where $R_{g0} = l_0/2$ for a uniform cube and $R_{g0} = R\sqrt{3/5}$ for a uniform ball. The limit $m \rightarrow \infty$ gives the radius of gyration of the ideal Cantor fractal

$$R_g = \frac{\sqrt{3}\beta_t l_0}{\sqrt{1 - \beta_s^2}}. \quad (30)$$

As expected, the characteristics of the ideal fractal do not depend on specific shapes from which the fractal is constructed.

IV. FORMFACTOR OF THE POLYDISPERSE SETS

Here we study a specific kind of polydispersity, when the whole fractal is proportionally scaled and the scales are distributed. This implies that it is sufficient to consider the distribution of the fractal length in the above formulas. Then the distribution function $D_N(l)$ of the scatterer sizes can be considered in such a way that $D_N(l)dl$ gives the probability to find a fractal whose size falls within the interval $(l, l + dl)$. Then the intensity can be written as

$$I_m^{\text{poly}}(q) = \frac{\int_0^\infty \langle F_m^2(\mathbf{q}) \rangle V_m^2(l) D_N(l) dl}{\int_0^\infty V_m^2(l) D_N(l) dl}, \quad (31)$$

where V_m is the total volume of the m th approximant

$$V_m = l^3 (2\beta_s)^{3m}. \quad (32)$$

The influence of the particle size distribution on the intensity scattering curves is essentially determined by its broadness. Narrow distributions (i.e., lognormal, Schulz, Gauss) have no influence on the scattering exponent but control a smoothing of the intensity curve, reproducing the power law behaviour for a certain value of the variance, while broad ones can change even the scattering exponent [13].

In order to study this influence on scattering from the Cantor sets, we consider a lognormal distribution given by

$$D_N(l) = \frac{1}{\sigma l \sqrt{2\pi}} \exp \left[-\frac{(\ln(l/l_0) + \sigma^2/2)^2}{2\sigma^2} \right], \quad (33)$$

$$\sigma \equiv \sqrt{\ln(1 + \sigma_r^2)}.$$

Here l_0 and σ_r are the mean length and its relative variance, respectively, that is,

$$l_0 \equiv \langle l \rangle_D, \quad \sigma_r \equiv \sqrt{\langle l^2 \rangle_D - l_0^2} / l_0, \quad (34)$$

where $\langle \dots \rangle_D \equiv \int_0^\infty \dots D_N(l) dl$. One can see that the relative variance regulates the width of the distribution.

Figure 4 represents the scattering curves from the monodisperse and polydisperse Cantor set for the fourth iteration at $\gamma = 0.2$. The curves corresponding to polydisperse cases approach the monodisperse ones as the distribution width σ_r tends to zero. A smoothing of intensity curve (31) increases when the width of the distribution σ_r gets larger. The most interesting effect is changing the power law exponent from the fractal dimension D in the fractal region (26) to the usual Porod exponent 4 beyond the region. Here the intensity is approximately proportional to the scaled intensity of a generator, according to Eq. (28), thus giving the Porod law. One can see the well in the intermediate region $ql_0 \sim 1/\beta_s^m$ where the monodisperse curve is shifted up to the asymptotics $1/8^m$. The well becomes even more pronounced when the size of a generator gets smaller, compare Figs. 4b and 4c. At very small generator size, even plateau should appear here. Such a behaviour of the scattering intensity was observed experimentally [30]. A phenomenological approach was developed in Ref. [35] for studying various exponents in the scattering intensity.

Note that the appearance of the well or “shelf” between the fractal and Porod regions near the volume $1/N_m$ is a consequence of the general asymptotics $1/N_m$ of the fractal structure factor. Thus, the position of the “shelf” allows us to estimate the volume of particles that form the fractal, provided the total fractal volume is known (see discussion in Sec. III A).

Expanding Eq. (31) as a power series in q and integrating over the distribution, we arrive at the radius of gyration given by Eq. (29) or (30) multiplied by the factor $(1 + \sigma_r^2)^{1/2}$.

V. CONCLUSION

We propose a new model that generalizes the well-known one-dimensional Cantor set and is characterized by the dimensionless cut-off parameter. The parameter controls the fractal dimension, which can be varied from 0 to 3. The latter is over the standard for mass fractals from the experimental points of view [36]: the fractals dimensions less than 1 have not been observed yet. The formfactor of the generalized Cantor set is calculated analytically for arbitrary iteration. This allows us to evaluate the scattering intensity for monodisperse and polydisperse fractals by means of simple integrals. We find the values of asymptotics of the fractal structure factor and reveal their nature. The radius of gyration is obtained analytically as well.

The suggested model describes changing of the power law exponent from the fractal dimension to the usual Porod exponent beyond the fractal region. In the intermediate region a typical well or “shelf” arises, which can be observed in experiments [30]. In comparison with paper [16], we not only calculate the scattering intensity for large momenta but also explain its behaviour. Moreover, if an experiment observes the threshold between the fractal and Porod regions, the suggested approach yields the number of particles in the fractal set. Another way to describe the experimental data for frac-

tals is *ab initio* methods, see, e.g., Ref. [37].

In a number of cases we have *a priori* information about the fractal structure, for instance, when the fractal synthesis is well controlled by chemical methods. Then one can build a fractal model with many parameters. With the model, one can obtain an additional information from the scattering data. The generalized Cantor set is an example of such a construction. A similar scheme can be developed by the same methods for another type of fractal sets.

The model can be extended to match specific needs in various ways, including different values of the cut-off parameter at each iteration, different probability distributions for the

fractal length and the shapes from which it is constructed, and so on. The introduced models and methods can be useful for analyzing the scattering from new types of materials such as polymeric systems or soils.

Acknowledgments

The authors are grateful to A. N. Ozerin and V. I. Gordeliy for fruitful discussions.

-
- [1] L. A. Feigin and D. I. Svergun, *Structure Analysis by Small-Angle X-Ray and Neutron Scattering* (Plenum press, New York, London, 1987).
 - [2] T. Zemb and P. Lindner, *Neutron, X-Rays and Light. Scattering methods applied to soft condensed matter* (North Holland, Amsterdam, The Netherlands, 2002).
 - [3] O. Glatter and O. Kratky, *Small-angle X-ray Scattering* (Academic Press, London, 1982).
 - [4] P. Pfeifer and D. Avnir, *J. Chem. Phys.* **79**, 3558 (1983).
 - [5] B. Mandelbrot, *The Fractal Geometry of Nature* (W.H. Freeman, USA, 1983).
 - [6] P. Pfeifer and M. Obert, *The Fractal Approach to Heterogeneous Chemistry* (John Wiley and Sons Ltd, New York, 1989).
 - [7] H. Peitgen, H. Jurgens, and D. Saupe, *Chaos and Fractals: New Frontiers of Science 2nd ed.* (Springer Verlag, New York, 2004).
 - [8] A. I. Kuklin, A. V. Rogachev, A. Y. Cherny, E. B. Dokukin, A. K. Islamov, Y. S. Kovalev, T. N. Murugova, D. V. Soloviev, O. I. Ivankov, A. G. Soloviev, et al., *Do the size effects exist?*, arXiv.org:0908.3804 (2009).
 - [9] H. D. Bale and P. W. Schmidt, *Phys. Rev. Lett.* **53**, 596 (1984).
 - [10] S. Sinha, T. Freltoft, and J. Kjems, *Kinetics of Aggregation and Gelation* (North-Holland, Amsterdam, 1984).
 - [11] J. E. Martin and B. J. Ackerson, *Phys. Rev. A* **31**, 1180 (1985).
 - [12] T. Freltoft, J. K. Kjems, and S. K. Sinha, *Phys. Rev. B* **33**, 269 (1986).
 - [13] J. E. Martin, D. W. Schaefer, and A. J. Hurd, *Phys. Rev. A* **33**, 3540 (1986).
 - [14] A. J. Hurd, D. W. Schaefer, and J. E. Martin, *Phys. Rev. A* **35**, 2361 (1987).
 - [15] O. Malcai, D. A. Lidar, O. Biham, and D. Avnir, *Phys. Rev. E* **56**, 2817 (1997).
 - [16] P. W. Schmidt and X. Dacai, *Phys. Rev. A* **33**, 560 (1986).
 - [17] J. Kjems and P. Schofield, *Scaling Phenomena in Disordered Systems* (Plenum, New York, 1986), pp. 141–149.
 - [18] P. W. Schmidt, *J. Appl. Cryst.* **24**, 414 (1991).
 - [19] H. Mayama and K. Tsuji, *J. Chem. Phys.* **125**, 153 (2008).
 - [20] M. W. Takeda, S. Kirihara, Y. Miyamoto, K. Sakoda, and K. Honda, *Phys. Rev. Lett.* **92**, 093902 (2004).
 - [21] G. F. Cerofolini, D. Narducci, P. Amato, and E. Romano, *Nanoscale Research Letters* **3**, 381 (2008).
 - [22] D. Yamaguchi, H. Mayama, S. Koizumi, K. Tsuji, and T. Hashimoto, *Eur. Phys. J. B* **63**, 124706 (2006).
 - [23] G. R. Newkome, P. Wang, C. N. Moorefield, T. J. Cho, P. P. Mohapatra, S. Li, S.-H. Hwang, O. Lukoyanova, L. Echegoyen, J. A. Palagallo, et al., *Science* **312**, 1782 (2006).
 - [24] C. M. Sorensen and G. M. Wang, *Phys. Rev. E* **60**, 7143 (1999).
 - [25] P. Pfeifer, F. Ehrburger-Dolle, T. P. Rieker, M. T. González, W. P. Hoffman, M. Molina-Sabio, F. Rodríguez-Reinoso, P. W. Schmidt, and D. J. Voss, *Phys. Rev. Lett.* **88**, 115502 (2002).
 - [26] P. W. Schmidt, *Modern Aspects of Small-Angle Scattering, Ch.1, ed. H. Brumberger, NATO Science Series C, Vol. 451* (Springer, 1995).
 - [27] G. N. Fedotov, Y. D. Tret'yakov, E. I. Pakhomov, A. I. Kuklin, and A. K. Islamov, *Doklady Chem.* **407**, 51 (2006).
 - [28] G. N. Fedotov, Y. D. Tret'yakov, V. I. Putlyaev, E. I. Pakhomov, A. I. Kuklin, and A. K. Islamov, *Doklady Chem.* **412**, 55 (2007).
 - [29] G. N. Fedotov, E. I. Pakhomov, A. I. Pozdnyakov, A. I. Kuklin, A. K. Islamov, and V. I. Putlyaev, *Eurasian Soil Science* **40**, 956 (2007).
 - [30] D. V. Lebedev, M. V. Filatov, A. I. Kuklin, A. K. Islamov, J. Stellbrink, R. A. Pantina, Y. Y. Denisov, B. P. Toperverg, and V. V. Isaev-Ivanov, *Cryst. Rep.* **53**, 110 (2008).
 - [31] M. E. Dokukin, N. S. Perov, E. B. Dokukin, A. K. Islamov, A. I. Kuklin, Y. E. Kalinin, and A. V. Sitnikov, *Bull. Russ. Acad. Sci.: Physics* **71**, 1602 (2007).
 - [32] In the literature, the quantity $VF(q)$ is sometimes called scattering amplitude, while the squared and averaged quantity $V^2\langle|F(q)|^2\rangle$ is meant by formfactor.
 - [33] D. A. Hamburger-Lidar, *Phys. Rev. E* **54**, 354 (1996).
 - [34] In statistical mechanics, the structure factor is usually defined to be N_m times larger.
 - [35] G. Beaucage, *J. of Appl. Cryst.* **28**, 717 (1995).
 - [36] O. Malcai, D. A. Lidar, O. Biham, and D. Avnir, *Phys. Rev. E* **56**, 2817 (1997).
 - [37] A. N. Ozerin, A. M. Muzafarov, L. A. Ozerina, D. S. Zavorotnyuk, I. B. Meshkov, O. B. Pavlova-Verevskina, and M. A. Beshenko, *Doklady Chem.* **411**, 202 (2006).